Snowfall Type Classification for Improving Passive Microwave Snowfall Estimates

Lisa Milani[1,2], Veljko Petkovic[1,3], Marko Orescanin[4], Mark S. Kulie[5]

[1] Earth System Science Interdisciplinary Center (ESSIC), University of Maryland, College Park, MD.

[2] NASA Goddard Space Flight Center, Greenbelt, MD.

[3] Cooperative Institute for Satellite Earth System Studies (CISESS), University of Maryland, College Park, MD.

[4] Navy Postgraduate School, Monterey, CA, USA.

[5] NOAA/NESDIS/STAR/ASPB.

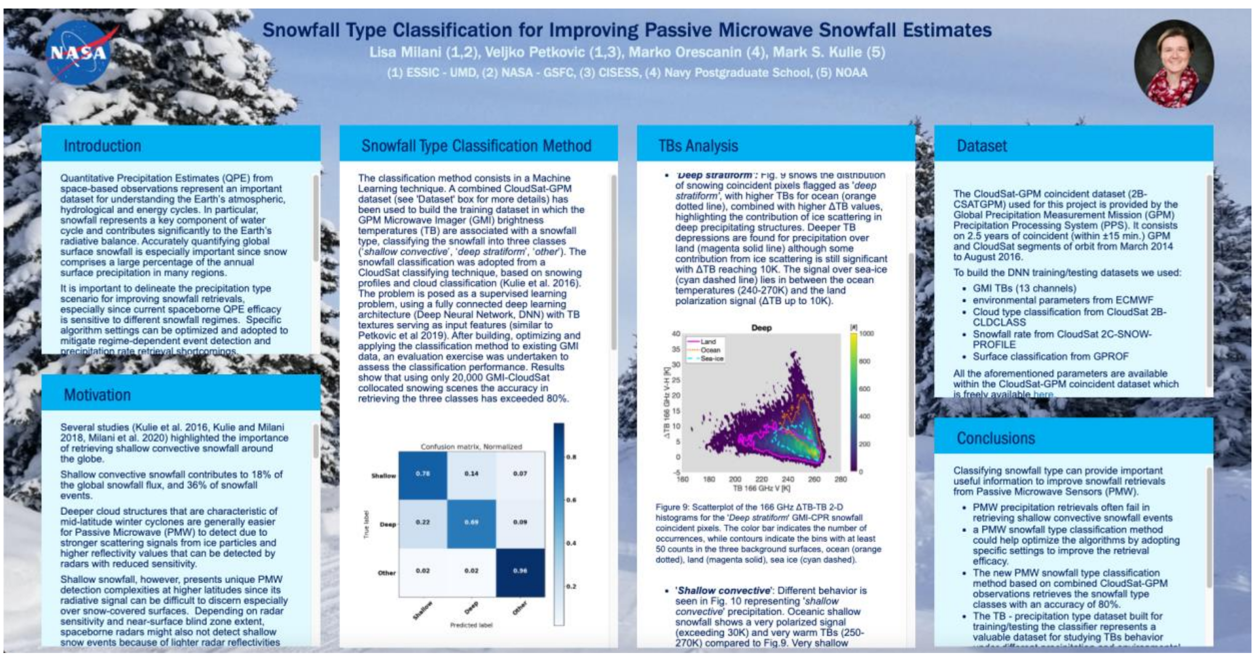

Introduction

Quantitative Precipitation Estimates (QPE) from space-based observations represent an important dataset for understanding the Earth's atmospheric, hydrological and energy cycles. In particular, snowfall represents a key component of water cycle and contributes significantly to the Earth's radiative balance. Accurately quantifying global surface snowfall is especially important since snow comprises a large percentage of the annual surface precipitation in many regions.

It is important to delineate the precipitation type scenario for improving snowfall retrievals, especially since current spaceborne QPE efficacy is sensitive to different snowfall regimes. Specific algorithm settings can be optimized and adopted to mitigate regime-dependent event detection and precipitation rate retrieval shortcomings.

This work aims to provide a flag classifying most common snowfall types, '*shallow cumuliform*' and '*deep stratiform*' representing together the 95% of the global snowfall fraction (Kulie et al. 2016).

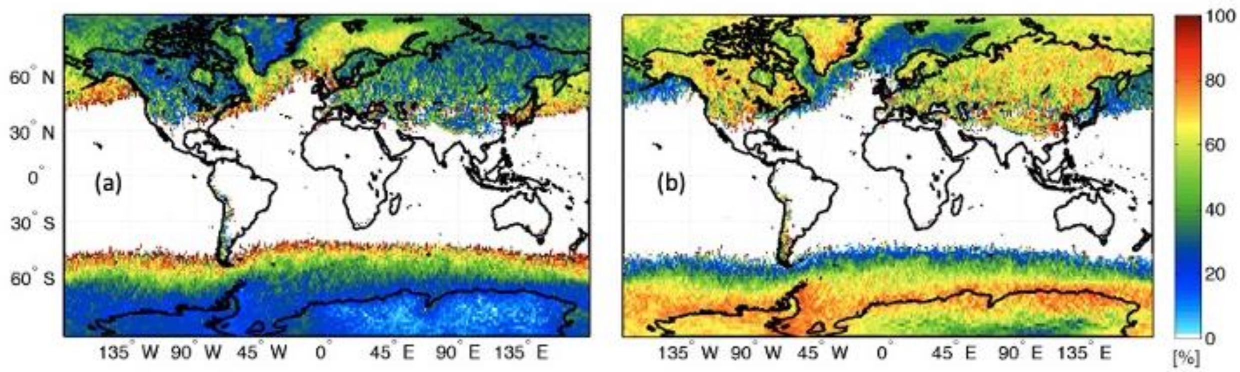

Figure 1: CloudSat observed (a) 'shallow cumuliform' and (b) 'deep stratiform' snowfall fraction (Kulie et al. 2016, ©Copyright 2016 American Meteorological Society).

Motivation

Several studies (Kulie et al. 2016, Kulie and Milani 2018, Milani et al. 2020) highlighted the importance of retrieving shallow convective snowfall around the globe.

Shallow convective snowfall contributes to 18% of the global snowfall flux, and 36% of snowfall events.

Deeper cloud structures that are characteristic of mid-latitude winter cyclones are generally easier for Passive Microwave(PMW) to detect due to stronger scattering signals from ice particles and higher reflectivity values that can be detected by radars with reduced sensitivity.
Shallow snowfall, however, presents unique PMW detection complexities at higher latitudes since its radiative signal can be difficult to discern especially over snow-covered surfaces. Depending on radar sensitivity and near-surface blind zone extent, spaceborne radars might also not detect shallow snow events because of lighter radar reflectivities and extremely shallow cloud tops.

Milani et al. (2020) analyzed these complexities over the US Great Lakes Region. Shallow, lake-induced convection can persist over the same area for days, accumulating large amounts of snow over neighboring land regions. Fig. 2 shows an example of shallow convective lake-effect snow event over Lake Erie and Ontario in a 10 hour animation.

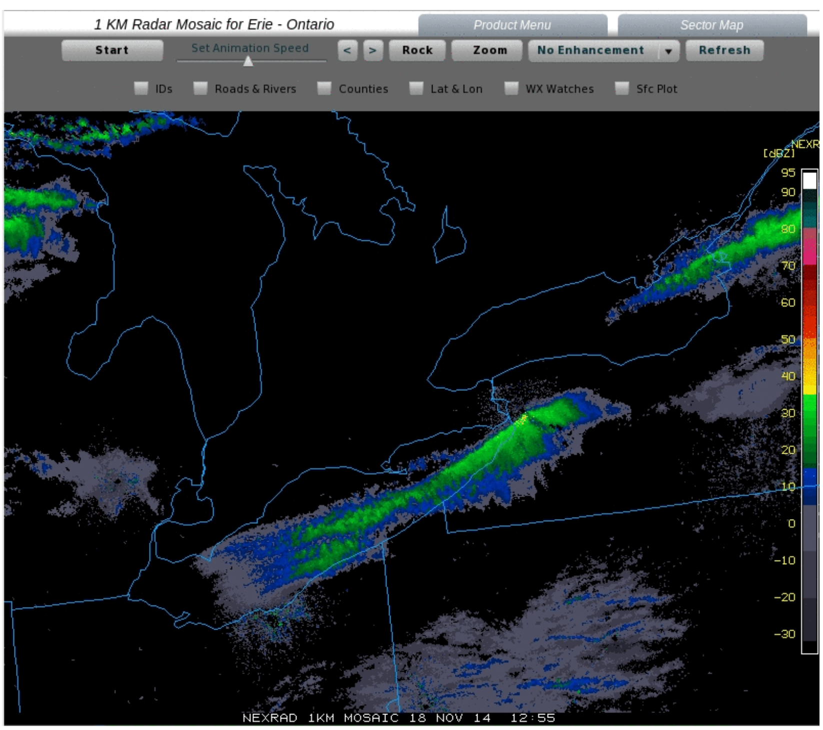

Figure 2: NEXRAD reflectivities on 18 November 2014 (12.55 to 23.00 UTC), animation credit CIMSS Satellite Blog (https://cimss.ssec.wisc.edu/satellite-blog/).

There is a strong distinctive high frequency (>89GHz) PMW signal associated with this type of event (Fig. 3 shows the Δ183.31GHz from the Global Precipitation Measurement (GPM) Microwave Imager (GMI)), but not always PMWQPE algorithms consistently detect and quantify the amount of snowfall.

Within the GPM mission, the Goddard PROFiling (GPROF) algorithm snowfall retrieval is the primary PMW precipitation product. GPROF estimates the probability of precipitation relying on a Bayesian approach using an a-priori knowledge to link the observed brightness temperature (TB) to the corresponding precipitation rates (Kummerowet al. 2015). GMI actually detects shallowsnow (Fig.3), but the a-priori database does not effectively translate TB's associated with shallow snow with reliable precipitation rates. For this reason GPROF generally underestimates both snowfall detection and quantification when compared to active remote sensing sensor snowfall products. Fig. 4 shows an example of precipitation estimates from the Multi-Radar/Multi-Sensors (GV-MRMS) ground validation product (Fig. 4a) and GPROF (Fig. 4b) over the Lake Erie and Ontario region on9 January 2015

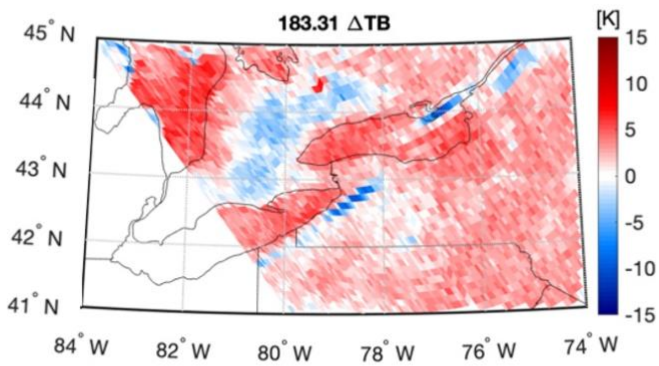

Figure 3: GMI 183.3±7 - 183.3±3 GHz TB differences for the GPM-Core Observatory overpass near 1226 UTC 9 January 2015 (Orbit #4914) (Milani et al. 2020, ©Copyright 2020 American Meteorological Society).

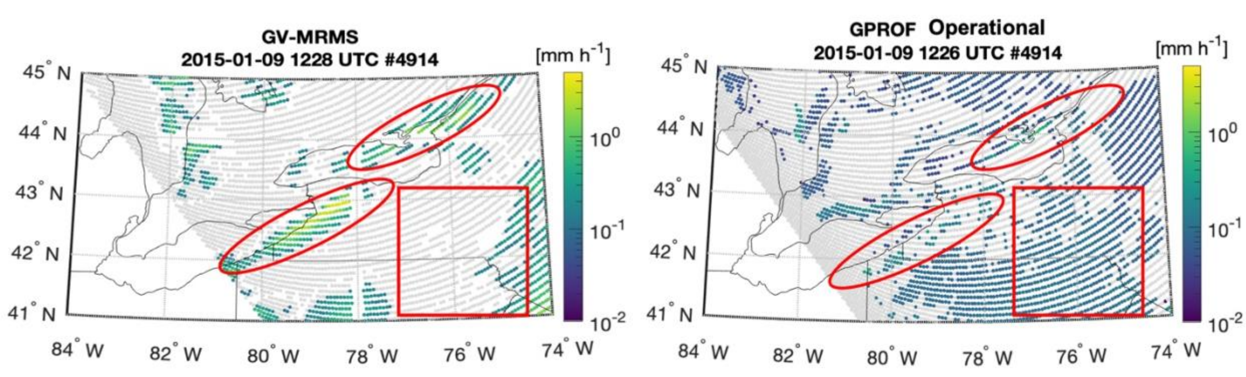

Figure 4: (a) GV-MRMS snowfall rate over Lakes Erie and Ontario on 9 January 2015 at 1226 UTC (orbit #4914), (b) GPROF precipitation rate(using SurfPrecip parameter from the Operational product) (Milani et al. 2020, ©Copyright 2020 American Meteorological Society).

GPROF clearly does not detect the snow bands over the lakes and the coastal regions (Fig.4 circles), adding precipitation over snow covered surfaces instead (Fig.4 square).
These and similar issues motivated this research team to investigate a useful and efficient way to help a PMW algorithm detecting and retrieving shallow convective frozen precipitation.

Snowfall Type Classification Method

The classification method consists in a Machine Learning technique. A combined CloudSat-GPM dataset (see 'Dataset' box for more details) has been used to build the training dataset in which the GPM Microwave Imager (GMI) brightness temperatures(TB) are associated with a snowfall type, classifying the snowfall into three classes (‘*shallow convective’*, ‘*deep stratiform’*, ‘*other*’). The snowfall classification was adopted from a CloudSat classifying technique, based on snowing profiles and cloud classification (Kulie et al. 2016). The problem is posed as a supervised learning problem, using a fully connected deep learning architecture (Deep Neural Network, DNN) with TB textures serving as input features (similar to Petkovic et al 2019). After building, optimizing and applying the classification method to existing GMI data, an evaluation exercise was undertaken to assess the classification performance. Results show that using only 20,000 GMI-CloudSat collocated snowing scenes the accuracy in retrieving the three classes has exceeded 80%.

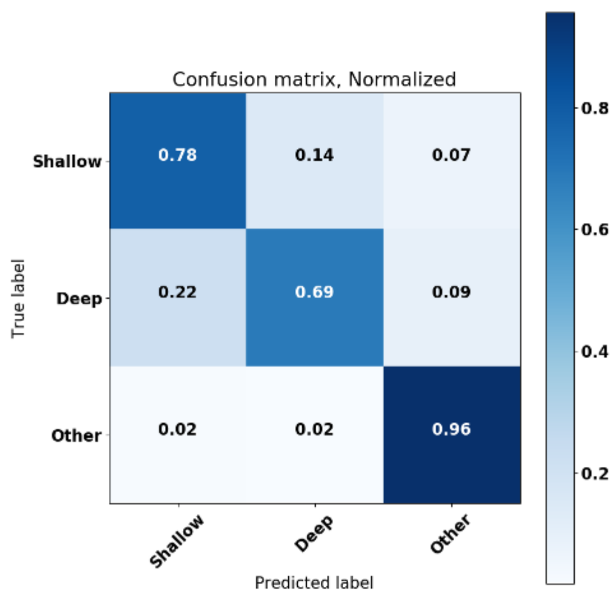

Figure 5: Accuracy of the DNN model CloudSat snow class retrieval. Confusion matrix for three snow classes (‘shallow convective’, ‘deep stratiform’ and ‘other’).

To build the training dataset, we adopted the classification algorithm developed by Kulie et al. (2016). The two main snowfall classes can be described as:

- ***'Deep stratiform'***: snowfall is associated with nimbostratus cloud structures. The nimbostratus normalized cloud thickness distribution is broad and centered around 4–5 km (Fig. 8).

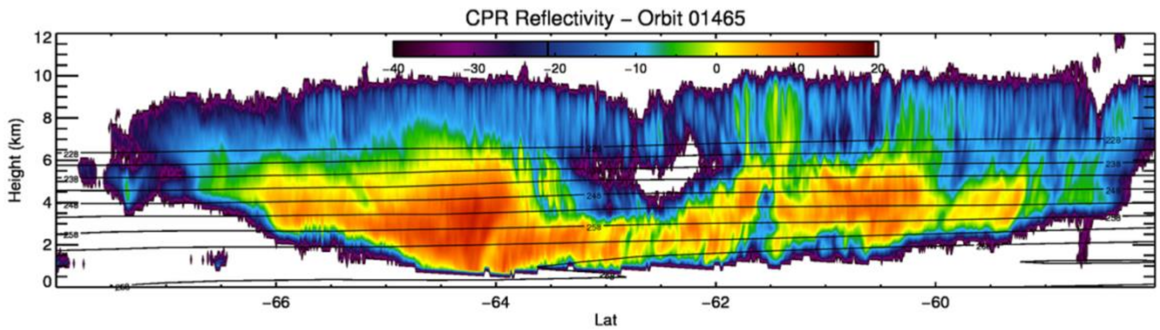

Figure 6: example of 'Deep stratiform' CloudSat reflectivity vertical profile.

- ***'Shallow cumuliform'***: snowfall is associated with cumulus and stratocumulus, is produced from very shallow cumuliform clouds (from which the name) with cloud thickness mostly less than 3 km (the cloud thickness distribution is centered around 1-2 km, fig. 8).

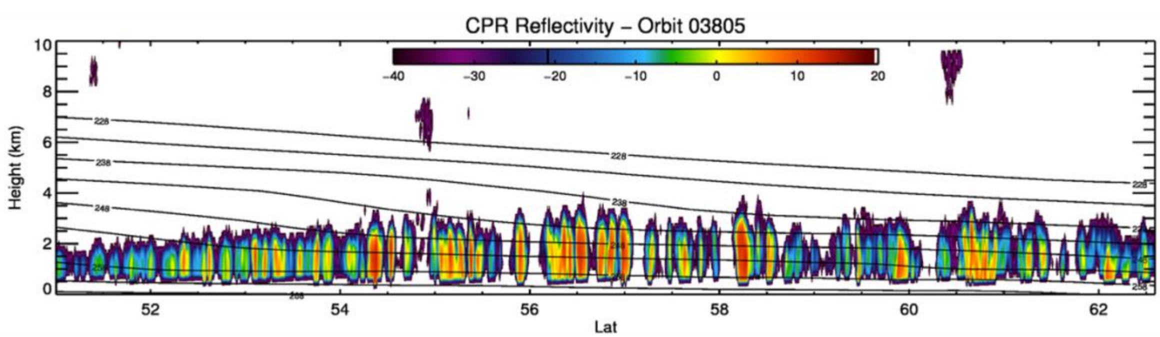

Figure 7: example of 'Shallow convective' CloudSat reflectivity vertical profile.

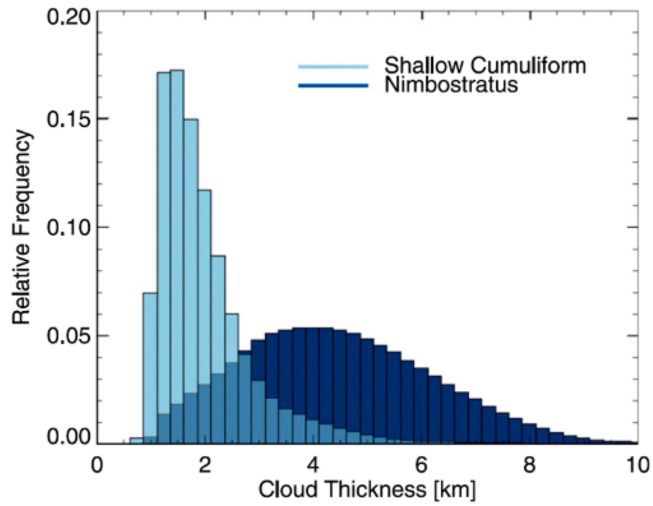

Figure 8: Cloud-top thickness distributions associated with shallow cumuliform (light blue) and nimbostratus (dark blue) CloudSat snowfall-producing cloud structures. Shallow vs deeper nimbostratus snowfall categories are defined by the CloudSat 2B-CLDCLASS product, while cloud thicknesses are calculated from the 2B-GEOPROF and 2C-PRECIP-COLUMN products (see Kulie et al. 2016 for details, ©Copyright 2016 American Meteorological Society).

TBs Analysis

The training/testing dataset built for the classifier (see 'Dataset' box for more details), also represents a very valuable dataset for investigating multi-frequency TB behavior under different snowfall type conditions. Panegrossi et al. (2017) introduced the TB analysis using a similarly built coincident dataset. We started from Panegrossi et al. (2017) results and partitioned the coincident dataset into sub-datasets to investigate possible unique signatures of TBs and TB differences (ΔTB) based on snowfall modes.

Figures 9 and 10 show the 2D histograms of the coincident dataset in the 166 GHz TB-ΔTB 2-D space. Similar to Panegrossi et al. (2017), we found positive 166 GHz ΔTB (V-H) with TBs spanning between 200 and 270 K.

- ***'Deep stratiform'***: Fig. 9 shows the distribution of snowing coincident pixels flagged as 'deep stratiform', with higher TBs for ocean (orange dotted line), combined with higher ΔTB values, highlighting the contribution of ice scattering in deep precipitating structures. Deeper TB depressions are found for precipitation over land (magenta solid line) although some contribution from ice scattering is still significant with ΔTB reaching 10K. The signal over sea-ice (cyan dashed line) lies in between the ocean temperatures (240-270K) and the land polarization signal (ΔTB up to 10K).

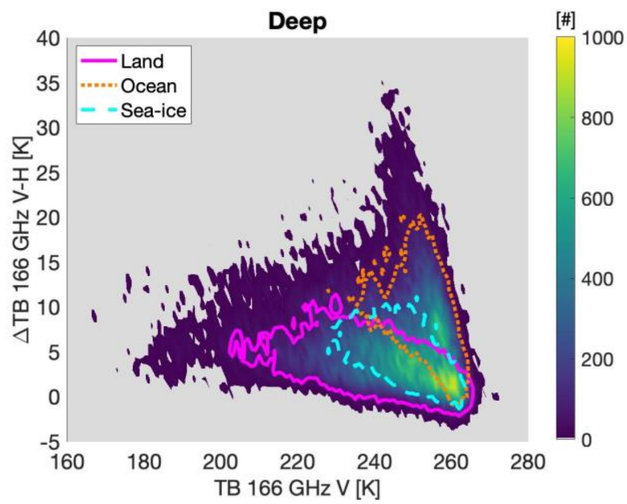

Figure 9: Scatterplot of the 166 GHz ΔTB-TB 2-D histograms for the 'Deep stratiform' GMI-CPR snowfall coincident pixels. The color bar indicates the number of occurrences, while contours indicate the bins with at least 50 counts in the three background surfaces, ocean (orange dotted), land(magenta solid), sea ice (cyan dashed).

- ***'Shallow convective'***: Different behavior is seen in Fig. 10 representing 'shallow convective' precipitation. Oceanic shallow snowfall shows a very polarized signal (exceeding 30K) and very warm TBs (250-270K) compared to Fig.9.Very shallow precipitation structures, combined with dry environmental conditions, allow the radiative signal to travel deeper through the atmosphere, with the very polarized oceanic surface contributing to the high ΔTB observed. For the same reason, the less polarized land surface, most likely covered by snow, contributes to the more variable 166GHz temperatures showing much less polarization (ΔTB<5K). Many shallow cumuliform snowfall events also contain ample supplies of supercooled cloud water that effectively tempers the ice scattering signature.

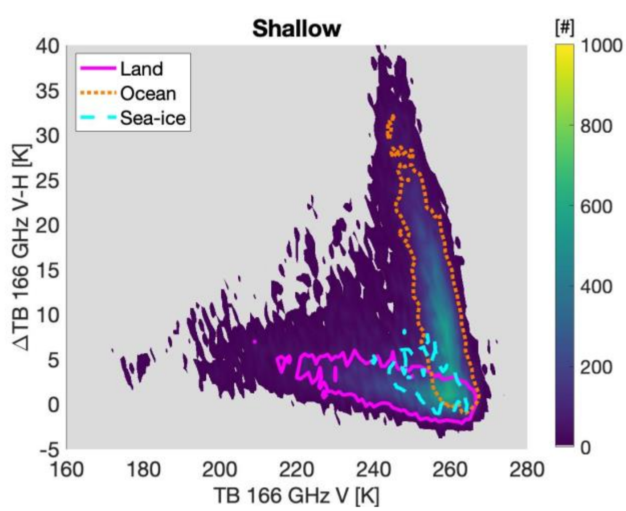

Figure 10: similar to Fig. 9 but for 'Shallow convective' pixels.

Other GMI channel combinations are being explored to better understand PMW signals associated with different snowfall regimes that depend on the complex interplay between microphysical composition (e.g., ice scattering versus supercooled cloud water emission), ambient water vapor content, and underlying surface type. The functional relationship between TB signal combinations with surface snowfall rate is also being investigated.

Dataset

The CloudSat-GPM coincident dataset (2B-CSATGPM) used for this project is provided by the Global Precipitation Measurement Mission (GPM) Precipitation Processing System (PPS). It consists on 2.5 years of coincident (within ±15 min) GPM and CloudSat segments of orbit from March 2014 to August 2016.

To build the DNN training/testing datasets we used:

- GMI TBs (13 channels)
- Environmental parameters from ECMWF
- Cloud type classification from CloudSat 2B-CLDCLASS
- Snowfall rate from CloudSat 2C-SNOW-PROFILE
- Surface classification from GPROF
-

All the aforementioned parameters are available within the CloudSat-GPM coincident dataset which is freely available here (https://gpm.nasa.gov/data).

Conclusions

Classifying snowfall type can provide important useful information to improve snowfall retrievals from Passive Microwave Sensors (PMW).

- PMW precipitation retrievals often fail in retrieving shallow convective snowfall events a PMW snowfall type classification method could help optimize the algorithms by adopting specific settings to improve the retrieval efficacy.
- The new PMW snowfall type classification method based on combined CloudSat-GPM observations retrieves the snowfall type classes with an accuracy of 80%.
- The TB - precipitation type dataset built for training/testing the classifier represents a valuable dataset for studying TBs behavior under different precipitation and environmental conditions (surface type, snowfall type, temperature, precipitable water etc.). Other GMI channel combinations are being explored to better understand PMW signals associated with different snowfall regimes.

References

Kulie, M. S., and Milani, L. (2018). Seasonal variability of shallow cumuliform snowfall: A CloudSat perspective. Quarterly Journal of the Royal Meteorological Society, 144(S1), 329-343, doi: 10.1002/qj.3222 (https://doi.org/10.1002/qj.3222).

Kulie, M. S., Milani, L., Wood, N. B., Tushaus, S. A., Bennartz, R., and L'Ecuyer, T. S. (2016). A shallow cumuliform snowfall census using spaceborne radar. Journal of Hydrometeorology, 17(4), 1261-1279, doi: 10.1175/Jhm-D-15-0123.1

Kummerow, C. D., Randel, D. L., Kulie, M., Wang, N. Y., Ferraro, R., Munchak, S. J., and Petkovic, V. (2015). The evolution of the Goddard PROFiling algorithm to a fully parametric scheme. Journal of Atmospheric and Oceanic Technology, 32(12),2265-2280, doi: 10.1175/jtech-d-15-0039.1

Milani, L., et al. (2020). Extreme lake-effect snow from a GPM microwave imager perspective: Observational analysis and precipitation retrieval evaluation. Journal of Atmospheric and Oceanic Technology, https://doi.org/10.1175/JTECH-D-20-0064.1

Panegrossi, G., Rysman, J.-F., Casella, D., Marra, A., Sanò, P., and Kulie, M. (2017). Cloudsat-based assessment of gpmmicrowave imager snowfall observation capabilities. Remote Sensing, 9(12), doi: 10.3390/rs9121263

Petković, V., M. Orescanin, P. Kirstetter, C. Kummerow, and R. Ferraro, 2019: Enhancing PMW Satellite PrecipitationEstimation: Detecting Convective Class. J. Atmos. Oceanic Technol., 36, 2349–2363, https://doi.org/10.1175/JTECH-D-19-0008.1